ELSEVIER

Thermochimica Acta 388 (2002) 159–173

thermochimica acta

www.elsevier.com/locate/tca

Thermal properties of DMNB, a detection agent for explosives

D.E.G. Jones*, P.D. Lightfoot, R.C. Fouchard, Q.S.M. Kwok

Canadian Explosives Research Laboratory, Natural Resources Canada, 555 Booth Street, Ottawa, Ont., Canada K1A 0G1

Received 6 June 2001; received in revised form 11 July 2001; accepted 11 July 2001

Abstract

The thermal behavior of 2,3-dimethyl-2,3-dinitrobutane (DMNB), a detection agent for explosives, was studied using various thermoanalytical techniques. Vapor pressure data for DMNB were obtained from differential scanning calorimetry (DSC) measurements. The enthalpy of sublimation for DMNB over different temperature ranges was estimated using DSC and dynamic and isothermal thermogravimetry (TG). Kinetic parameters for the decomposition of neat DMNB and DMNB in mesitylene solution were determined using various methods, and there was reasonable agreement between the results obtained for the solid and solution. Additionally, DSC and accelerating rate calorimetry (ARC) results at super-ambient pressures were compared to earlier heat flow calorimetry (HFC) results, and the effect of pressure on the thermal behavior of DMNB is also discussed.

Keywords: DMNB; Explosives detection agent; DSC; ARC; HFC

1. Introduction

Volatile detection agents are incorporated into plastic explosives at the point of manufacture in order to control their illegal transport. The International Civil Aviation Organization (ICAO) has specified certain detection agents [1]. 2,3-Dimethyl-2,3-dinitrobutane (DMNB) has been identified as the most suitable detection agent, as it does not affect explosive characteristics, such as shelf life and stability [2]. Our laboratory has conducted research on the thermal properties of DMNB and its mixtures with various explosive ingredients [2–7].

In this paper, the thermal behavior of DMNB was studied using differential scanning calorimetry (DSC), thermogravimetry (TG) and accelerating rate calorimetry (ARC). The vapor pressure and the enthalpy of sublimation for DMNB are reported. The kinetic parameters for thermal decomposition of neat DMNB and DMNB in mesitylene solution are presented. The high-pressure DSC and ARC results for DMNB are compared to earlier heat flow calorimetry (HFC) results [5], and the effect of pressure on the thermal behavior of DMNB is also discussed.

2. Experimental

DMNB and mesitylene were acquired from Aldrich and reported at >98 and 99 mol % purity, respectively. Both materials were used without further purification.

A TA 2100 Thermal Analysis System with 2910 DSC and 2950 TG modules was used with a nitrogen purge. Sealed glass microampoules were used in the DSC experiments conducted at ambient pressure and aluminium pans with laser-drilled pin-hole vented lids were

* Corresponding author. Tel.: +1-613-995-2140; fax: +1-613-995-1230.
E-mail address: djones@nrcan.gc.ca (D.E.G. Jones).

0040-6031/02/$ – see front matter
PII: S0040-6031(02)00033-3

used for measurements at pressure up to 6.9 MPa with a TA pressure cell. The details of the procedures for sample preparation and DSC measurements are described elsewhere [3]. The DSC was calibrated with respect to temperature [8] and heat flow [9]. The TG was calibrated for mass and temperature using a standard reference mass and the Curie point magnetic method [10].

The ARC is an adiabatic calorimeter distributed by Arthur D. Little Inc. The standard procedure of "heat-wait-search" was mostly used. Description of the thermokinetic information that can be obtained from ARC measurements [11] and a specific experimental procedure [12] have been published. Sample containers used for ARC experiments were titanium bombs. In addition to heat-wait-search experiments, some isothermal experiments were conducted between 418 and 433 K.

Note that the quoted uncertainties for all the results in this paper refer to one standard deviation and experimental scatter only. No attempt was made to quantify the uncertainties inherent in each method.

3. Results and discussions

A typical DSC curve for 0.7 mg of DMNB in a sealed glass microampoule [3] at a heating rate of 5 K min^{-1} is shown in Fig. 1. Three endothermic peaks were obtained at onset temperatures of 321 ± 2, 388 ± 2 and 475 ± 2 K. The peaks below 400 K correspond to two solid–solid phase transitions, and the third endotherm corresponds to the fusion of DMNB. The properties for the phase transformations of DMNB determined from our laboratory [3–5] and elsewhere [13,14] are summarized in Table 1.

3.1. Vapor pressure and enthalpy of sublimation

3.1.1. DSC

ASTM E 1782 [15] and E 2071 [16] were used to determine the vapor pressure and the enthalpy of sublimation from DSC results. According to the ASTM procedure [15], the pin-hole method can be used for the determination of the vapor pressure of solids. However, no specific examples of solids have been given, and there were no solid samples included in the interlaboratory test program. In order to confirm that the technique was capable of yielding reliable temperature and pressure data for the sublimation process, anthracene was used as a standard to test the procedure. The results show that the enthalpy of sublimation obtained from DSC agreed with the literature value for anthracene within the estimates of the uncertainties [17].

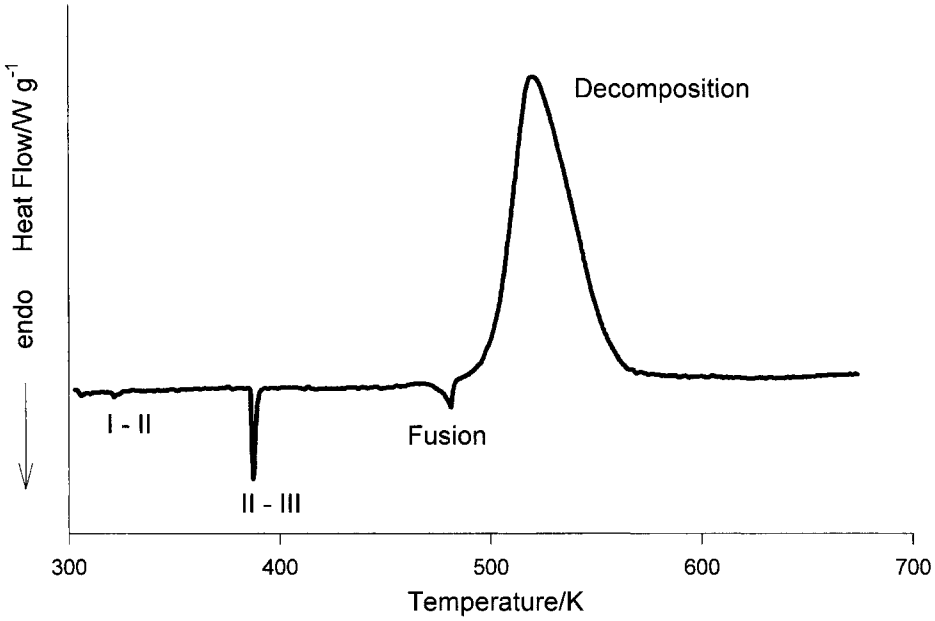

Fig. 1. DSC curve for DMNB in a microampoule at $\beta = 5$ K min^{-1}.

Table 1
Thermodynamic data for phase transformations in DMNB

Phase change	Method	T/K	ΔH/kJ mol^{-1}
I–II	DSC [3]	321 ± 2	1.0 ± 0.2
	HFC [5]	323 ± 2	0.95 ± 0.07
	DTA [14]	318 ± 5	0.6 ± 0.2
II–III	DSC [3]	388 ± 2	18 ± 2
	HFC [5]	388 ± 2	18 ± 2
	DTA [14]	388 ± 1	23 ± 2
Fusion	$\Delta_{\text{form}}H$ data [3]	473	15 ± 3
	Solubility [13]	275–308	29
	DSC + deconvolution [4]	473 ± 5	8.8 ± 0.5
	DSC (2.1–6.8 MPa)	480 ± 2	7.5 ± 0.8
Sublimation	Vapor pressure GC [13]	253–323 (phase I)	94
	Knudsen effusion [14]	303–330 (phases I and II)	85 ± 2
	Isothermal TG	323–353 (phase II)	74 ± 3
	Dynamic TG	340–380 (phase II)	74 ± 1
	DSC ASTM E 2017	420–478 (phase III)	63.1–63.9
Vaporization	$\Delta H_{\text{sub}}-\Delta H_{\text{fus}}$ DSC [3]	473	48 ± 3
	$\Delta H_{\text{sub}}-\Delta H_{\text{fus}}$ GC [13]	308	65
	$\Delta H_{\text{sub}}-\Delta H_{\text{fus}}$ DSC	473	55 ± 1

For the vapor pressure study of DMNB, DSC results collected between 3.3 and 34 kPa were used. The sublimation endotherm overlaps with those endotherms arising from (i) the II−III phase transition at 388 K below 3.3 kPa and (ii) fusion at 473 K above 34 kPa, thus preventing determination of the vapor pressure of DMNB in these ranges. Application of the Clausius–Clapeyron equation to the vapor pressure data resulted in the following vapor pressure equation:

$$\ln p = (19.4 \pm 0.2) - \frac{(7638 \pm 90)}{T}$$

The vapor pressure data are compared with the results obtained by Elias [13] and Smirnov et al. [14] in Fig. 2. In Elias' studies, gas chromatographic (GC) data from 253 to 323 K give:

$$\ln p = 29.53 - \frac{11248}{T}$$

and in Smirnov's studies, results from the Knudsen effusion method between 303 and 330 K give:

$$\ln p = 28.00 - \frac{10210}{T}$$

From these equations, enthalpies of sublimation of 93 and 85 ± 2 kJ mol^{-1} were obtained, respectively. The DSC results are significantly different from that obtained by GC or the Knudsen effusion method. As there is a significant difference in the temperature range, and DMNB is in a different crystalline form in each of these temperature ranges, a difference in the enthalpy of sublimation is expected. An example of the variation of ΔH_{sub} with crystalline form is demonstrated by white and red phosphorus [18].

In accordance with ASTM E 2071 [16], a fit of the vapor pressure data of DMNB to the Antoine equation:

$$\ln p = 18.60 - \frac{6969}{T - 20}$$

and the Clausius–Clapeyron approximation of the difference in compressibility upon sublimation ($\Delta Z_{\text{s}} = 1$) were used to estimate the enthalpy of sublimation between 420 and 480 K. The variation of ΔH_{sub} with temperature is illustrated in Fig. 3.

3.1.2. TG

The enthalpy of sublimation of DMNB was also estimated using a TG method described by Ohiyama and Wahlbeck [19]. This method involves determination of the rate of mass loss at a specific heating rate, and estimating the enthalpy of sublimation from the slope of a plot of $-\ln(\mathrm{d}m/\mathrm{d}t)$ against $1/T$. Typical

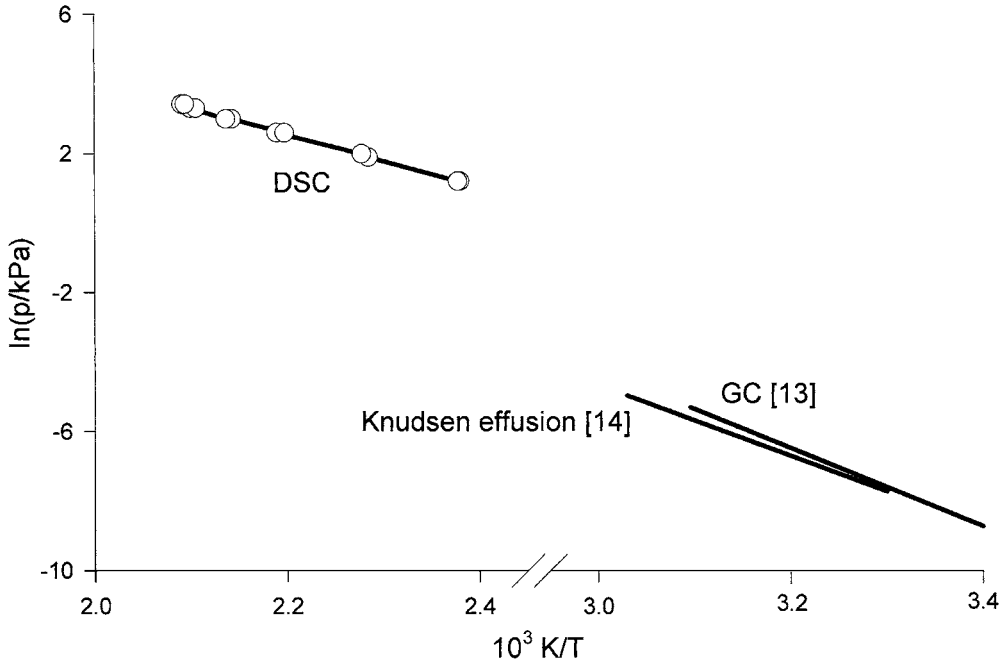

Fig. 2. Comparison of DSC, GC and Knudsen effusion vapor pressure results.

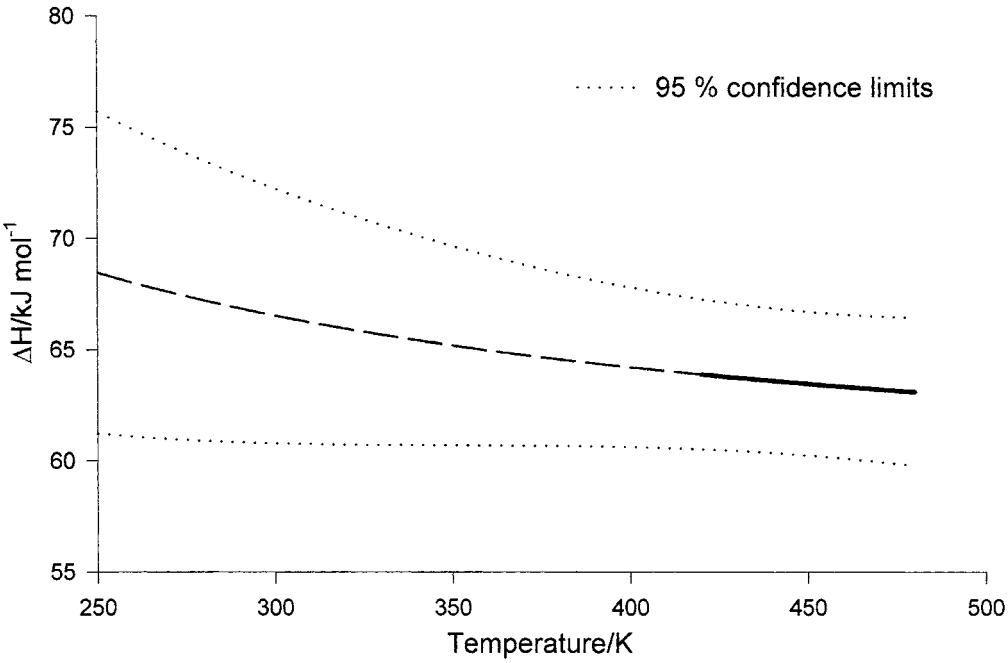

Fig. 3. ΔH_{sub} of DMNB. Solid line: DSC results; dashed line: extrapolated value.

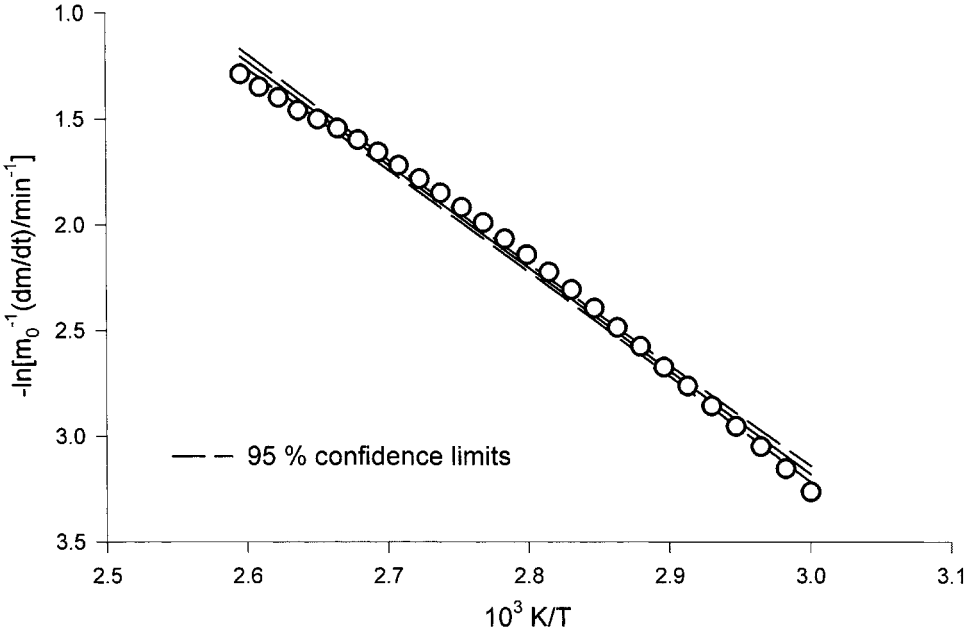

Fig. 4. Dynamic TG results to determine ΔH_{sub} of DMNB at $\beta = 2$ K min^{-1}.

results obtained for DMNB at temperatures between 340 and 380 K at a heating rate of 2 K min^{-1} are illustrated in Fig. 4. The enthalpies of sublimation derived from TG results at various heating rates ($\beta = 2$, 5 and 10 K min^{-1}) are listed in Table 2. An enthalpy of sublimation of 74 ± 1 kJ mol^{-1} was obtained by extrapolating to $\beta = 0$.

The sublimation of pharmaceutical compounds has been studied using isothermal TG [20]. The sublimation rate was measured directly from the mean mass loss per unit time in the linear region of the monitored TG profile at a set isothermal temperature. The results for DMNB at temperatures between 323 and 353 K are shown in Fig. 5, and an enthalpy of sublimation of 74 ± 3 kJ mol^{-1} was obtained from the data.

The enthalpies of sublimation obtained from dynamic (340–380 K) and isothermal (323–353 K) TG studies are similar, but different from that obtained by DSC (420–478 K). As discussed earlier, a difference in the enthalpy of sublimation is expected for DMNB in different temperature ranges, especially since DMNB is in a different crystalline form in each of these ranges. As compared in Table 1, there is a correlation between the ΔH_{sub} and the phase involved, and it seems that the value of ΔH_{sub} decreases as DMNB transforms through phases I–II–III. As shown in Fig. 3, ΔH_{sub} is expected to decrease as the temperature increases; however, the results obtained from GC [13], Knudsen effusion method [14], isothermal and dynamic TG are significantly higher than the extrapolated values for the corresponding temperature range. Thus, there is a true difference in the enthalpy of sublimation for DMNB in the different phases.

Table 2
ΔH_{sub} at various heating rates

β/K min^{-1}	ΔH_{sub}/kJ mol^{-1}
2	70.6 ± 0.8
5	67.1 ± 0.2
10	58.6 ± 0.1

3.2. Decomposition of DMNB

3.2.1. Decomposition of neat DMNB

As illustrated in Fig. 1, a large exotherm resulting from the decomposition was observed with an onset temperature of ~490 K from the DSC results for DMNB sealed in a glass microampoule. However, when the DSC measurements were conducted using

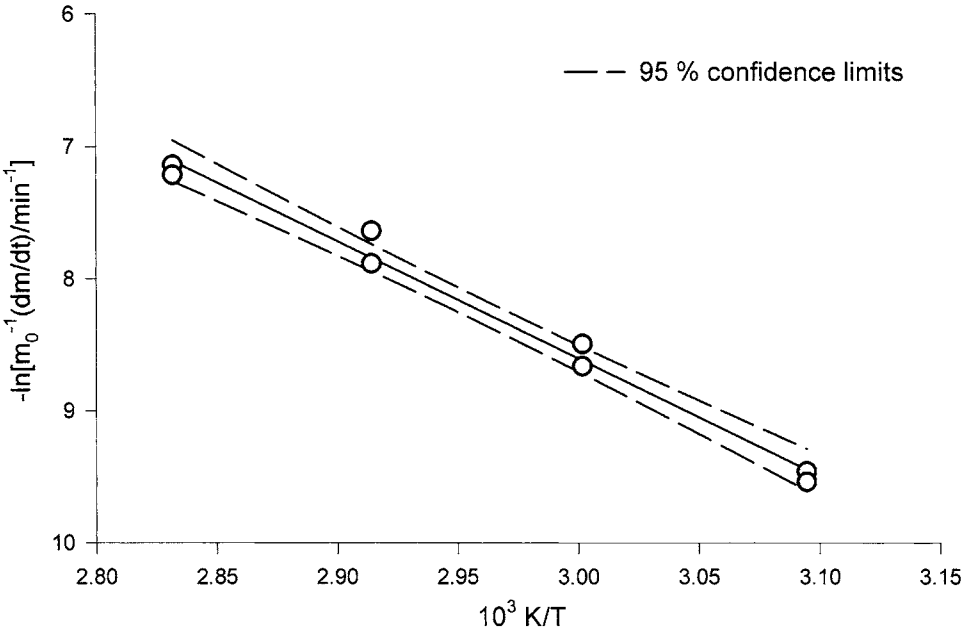

Fig. 5. Isothermal TG results to determine ΔH_{sub} of DMNB.

Al hermetic pans with pin-hole lids, no exotherm was observed at ambient pressure up to 573 K. At elevated pressure (2.1–6.9 MPa) of nitrogen, significant decomposition occurs in the vented pan system. The high-pressure DSC results (with vented pans) for 2.3 or 5 mg of DMNB are compared with the results obtained from the microampoule system in Table 3. The enthalpy change for the decomposition is less than that observed in the microampoule system, but appears to be pressure dependent in the vented pan system.

Decomposition of DMNB observed in conjunction with the melting endotherm (Fig. 1) suggests that the DMNB decomposition is initiated by the presence of the liquid phase. However, earlier HFC results [5] show that decomposition occurs prior to fusion. Additionally, substantial vapor pressure (estimated as about 26 kPa at 473 K) is present prior to the decomposition exotherm. Apparently, the decomposition of DMNB starts in the solid and/or gas phases.

Jones et al. [3] have described the results from a series of dynamic and isothermal DSC studies with microampoules to determine the kinetic parameters based on the Arrhenius equation. The dynamic DSC results were analyzed using ASTM E 698 [21], and the results of isothermal studies were analyzed in terms of both the *n*th-order model:

$$\frac{d\alpha}{dt} = k(1-\alpha)^n \quad (1)$$

and the autocatalytic model:

$$\frac{d\alpha}{dt} = k\alpha^m(1-\alpha)^n \quad (2)$$

where α is the fraction of sample decomposed, and n and m are the reaction orders. The dynamic and isothermal DSC results for DMNB are summarized in Table 4. It has been found that the simple *n*th-order model is statistically more significant than the autocatalytic model for the DSC isothermal results [3]. The isothermal results suggest an overall order significantly less than unity. The enhanced rate over that expected for a first-order process may be a direct result of the increased pressure of DMNB in the microampoule, since there is a significant vapor pressure of DMNB above 323 K.

The dynamic DSC results were also analyzed using the IsoKin isoconversional data analysis program [22]. The method implemented in this program takes its origin from the isoconversional method developed by

Table 3
Comparison of results for DMNB decomposition in various systems

System	Mass/mg	p/MPa	T_{onset}/K	$-\Delta H$/kJ mol^{-1}
DSC glass microampoule [3]	0.7		~490[a]	540 ± 40
DSC aluminum pan with pin-hole	5	2.1	~490[a]	246 ± 35
lid (nitrogen)	5	6.9		370 ± 18
	2.3	3.5		222 ± 2
	2.3	6.9		264 ± 18
ARC (argon)	250	0.1	448 ± 5[b]	(303)
	500	0.1	440 ± 5[b]	–
	1500	0.1	434 ± 5[b]	–
	250	3.5	444 ± 5[b]	(613)
ARC (air)	250	0.1	443 ± 5[b]	(482)
	250	3.5	423 ± 5[b]	–
HFC (air) [5]	40	0.1	430 ± 7[c]	443 ± 63
		5.5	423 ± 5[c]	>3700

The values in parentheses are estimated.
[a] Overlapped with fusion endotherm.
[b] Extrapolated to self-heating rate = 0.
[c] Temperature at which a deflection from the established baseline is observed.

Table 4
Decomposition results for DMNB, neat and in mesitylene solution

Method	E/kJ mol^{-1}	ln Z/min^{-1}	n	m
DMNBs				
DSC ASTM E 698 [3]	155 ± 7	34.4 ± 0.1	(1)	–
Isothermal DSC—Eq. (1) [3]	161 ± 9	36 ± 2	0.6 ± 0.1	–
Isothermal DSC—Eq. (2) [3]	100 ± 30	31 ± 8	0.7 ± 0.1	0.15 ± 0.1
Isoconversional analysis ($0.3 < \alpha < 0.7$)	151 ± 13	–	–	–
ARC—Eq. (3)				
0.25 g in ambient Ar	144 ± 10	31 ± 2	0.9 ± 0.1	–
0.25 g in 3.5 MPa Ar	122 ± 3	25 ± 1	1.6 ± 0.1	
0.25 g in ambient air	124 ± 5	26 ± 1	1.5 ± 0.1	–
ARC—linear				
0.25 g in ambient Ar	123 ± 3	29 ± 1	–	–
0.5 g in ambient Ar	172 ± 7	43 ± 2	–	–
1.5 g in ambient Ar	197 ± 10	51 ± 2	–	–
0.25 g in 3.5 MPa Ar	136 ± 1	33 ± 1	–	–
0.25 g in ambient air	124 ± 16	30 ± 4	–	–
0.25 g in 3.5 MPa air	186 ± 1	48 ± 1	–	–
ARC—isothermal				
1.5 g in ambient Ar	149 ± 13	–	–	–
20 mass % DMNB in mesitylene solution				
DSC ASTM E 698 [4]	133 ± 4	28.7 ± 0.1	(1)	–
Isothermal DSC—Eq. (1) [4]	133 ± 14	29 ± 3	≈0.2	–
Isothermal DSC—Eq. (2)	160 ± 20	31 ± 5	1.3 ± 0.2	0.9 ± 0.3
Isoconversional analysis ($0.3 < \alpha < 0.7$)	138 ± 5	–	–	–
ARC—Eq. (3) [12]	130 ± 30	27 ± 10	1.5 ± 0.1	–
ARC—linear [4]	121 ± 8	29 ± 2	–	–

The values in parentheses represent assumption.

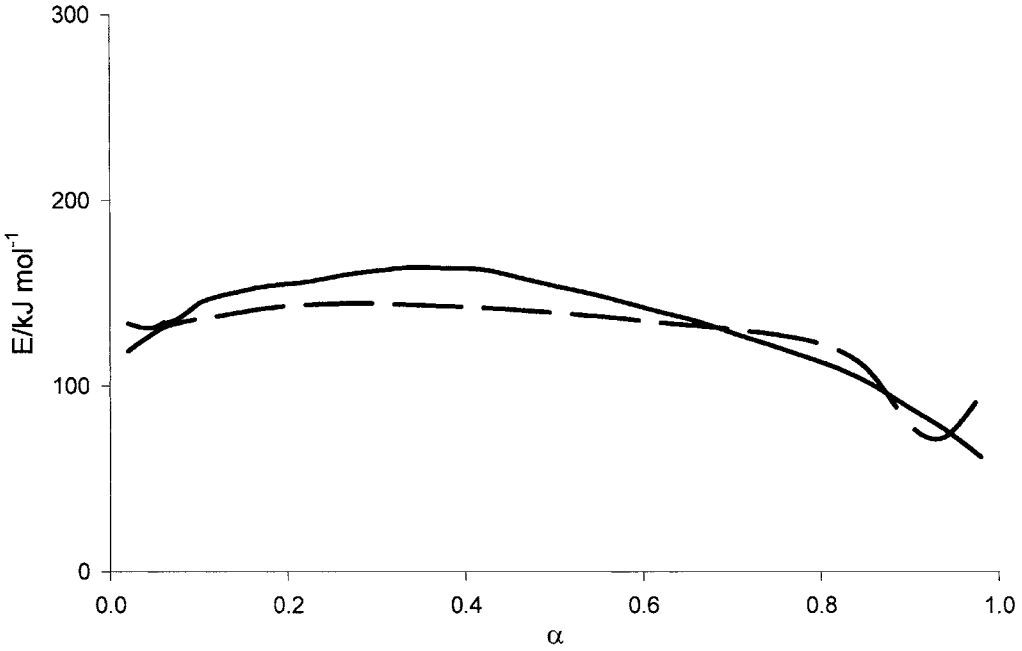

Fig. 6. Activation energy as a function of extent of reaction for DMNB decomposition. Solid line: neat DMNB; dashed line: 20 % DMNB solution.

Vyazovkin [23]. This method allows the estimation of the activation energy as a function of extent of reaction (α), and no assumptions about the kinetic model for the reaction are required [24–26]. As illustrated in Fig. 6, the results show that the activation energy is essentially independent of α for $0.3 < \alpha < 0.7$. The constancy of activation energy suggests that there is no major change in the decomposition mechanism over the exotherm. An average value of the activation energy obtained between $0.3 < \alpha < 0.7$ is listed in Table 4, and the average value is consistent with that found by ASTM E 698.

The thermal decomposition of DMNB was also studied using ARC. Results from a typical ARC experiment started at ambient pressure of argon, using 0.25 g of DMNB, are illustrated in Fig. 7. The 'true' onset temperature (extrapolated to self-heating rate = 0) is 448 ± 5 K. The lower onset temperature observed in the ARC experiments is a result of the larger sample size and lower heat losses compared to the DSC experiments.

Fig. 8 depicts the results obtained for 0.25 g of DMNB, when the rate data are analyzed in term of a *n*th-order reaction and the Arrhenius equation, as described by Jones and Fouchard [12], using equation:

$$\ln[R(t)] = n \ln[T_f - T(t)] - \frac{E}{RT(t)} + \ln\left[\frac{Z}{\Delta T^{n-1}}\right] \quad (3)$$

where n is the reaction order, T_f and T_i are the final and initial temperatures, respectively, when the self-heating rate = 0.02 K min^{-1}, and $\Delta T = T_f - T_i$. Values of $E = 144 \pm 10$ kJ mol^{-1}, $\ln(Z/\text{min}^{-1}) = 31 \pm 2$ and $n = 0.9 \pm 0.1$ were obtained.

For 0.5 and 1.5 g of DMNB in ambient pressure of argon, the 'true' onset temperatures are 440 ± 5 and 434 ± 5 K, respectively. As expected, the onset temperature appears to decrease as the sample mass increases, due to an increase in ratio of the thermal mass of DMNB to that of the ARC bomb. In these experiments, the self-heating rates exceeded 10 K min^{-1}, set as one of the criteria for the instrument to terminate a run. Consequently, the experiments were stopped automatically before the exotherms were completed. Accordingly, the kinetic parameters were estimated by analyzing the data for the initial period of the decomposition for which the plot in Fig. 8 is linear. The results are listed in Table 4.

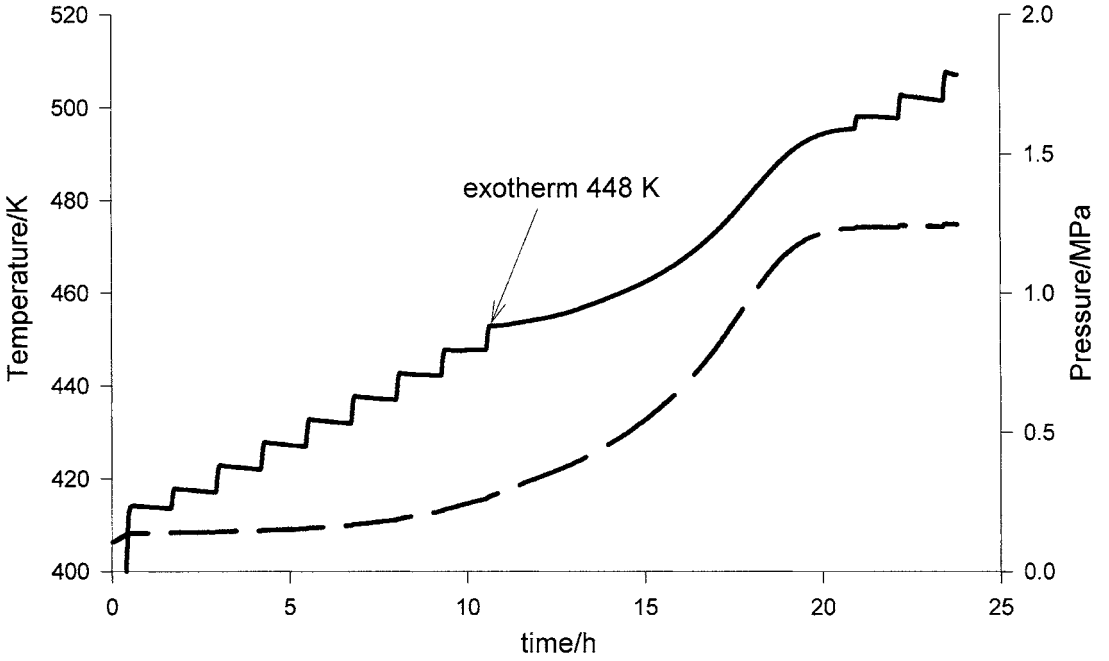

Fig. 7. ARC results for 0.25 g of DMNB in ambient pressure of argon. Solid line: temperature; dashed line: pressure.

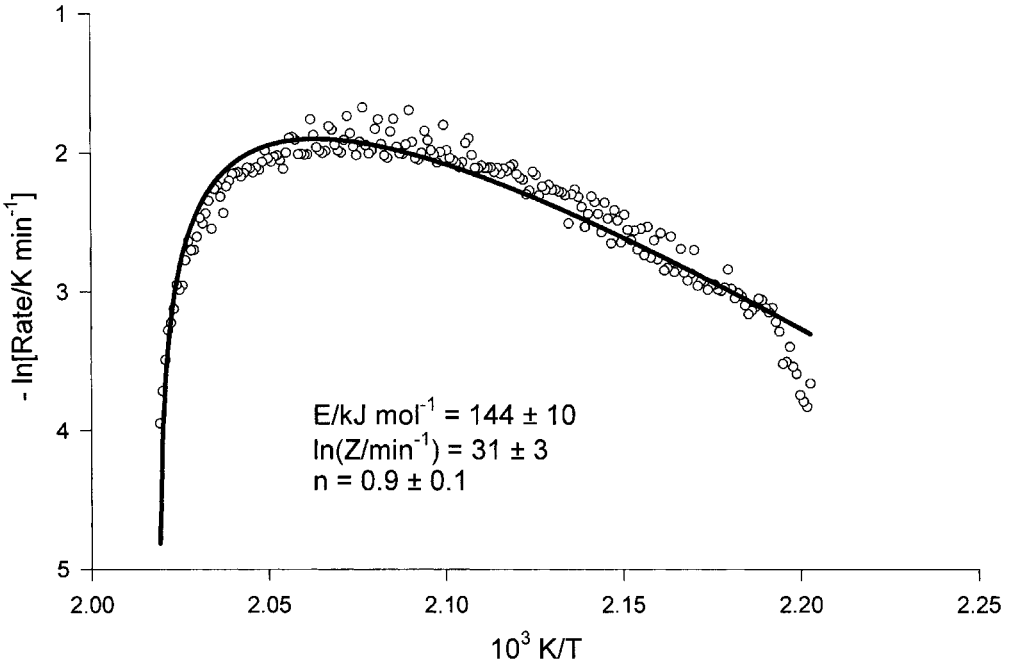

Fig. 8. ARC results for 0.25 g of DMNB according to Eq. (3).

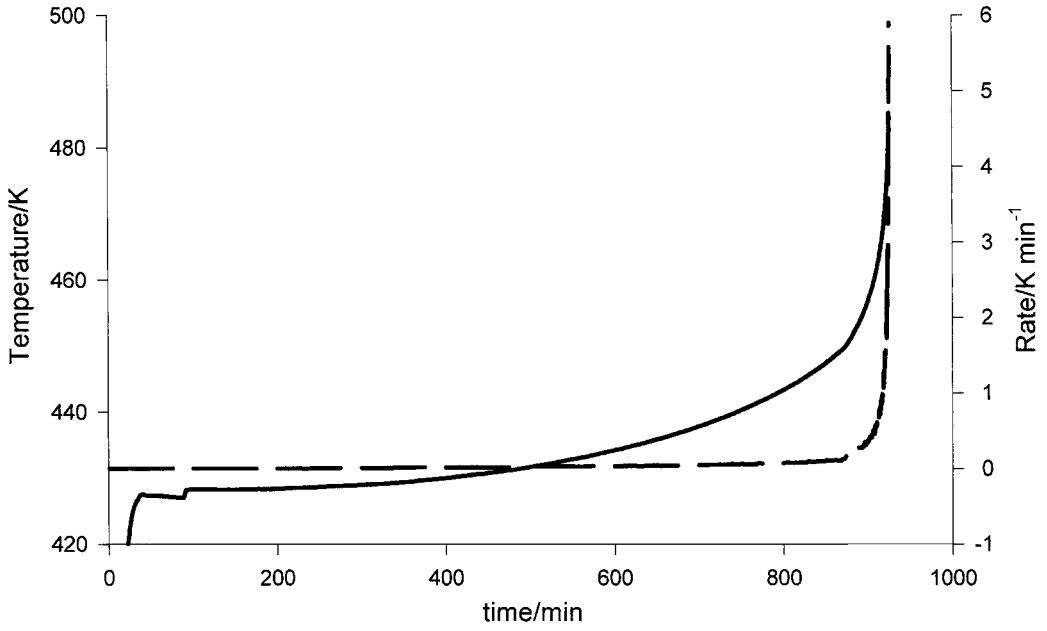

Fig. 9. ARC isothermal results at a nominal temperature of 428 K. Solid line: temperature; dashed line: pressure.

Additionally, the thermal decomposition of DMNB was studied using ARC isothermal studies. The results for DMNB at a nominal temperature of 428 K are illustrated by Fig. 9. Similar results were obtained for temperatures of 418–433 K. The time when the self-heating rates exceeded the maximum rate of automatic termination (5 K min^{-1}), τ (min) was estimated for each experiment. A value of $E = 149 \pm 13$ kJ mol^{-1} was determined from a plot of $\ln \tau$ versus the isothermal temperature, as shown in Fig. 10.

In order to further study the effect of pressure on the thermal behavior of DMNB, ARC experiments started at ambient and 3.5 MPa of argon or air were also conducted. The results are summarized in Tables 3 and 4. For 0.25 g of DMNB in 3.5 MPa of argon or ambient air, the onset temperature and the kinetic parameters are similar to those obtained from the ARC results for ambient argon.

The onset temperature and the kinetic parameters obtained from ARC experiment started at 3.5 MPa of air are significantly different from those obtained from argon or ambient air. The onset temperature of 423 ± 5 °C is similar to the earlier HFC results obtained in 5.5 MPa of air [5]. The enthalpy change obtained from HFC experiments started at 5.5 MPa of air is greater than 3.7 MJ mol^{-1}, which is close to the enthalpy of combustion of DMNB (3.8 MJ mol^{-1}) [14]. At 5.5 MPa, the amount of oxygen in the HFC system (5 cm^3 internal vessel volume) was 74 mg, which exceeded the required amount of oxygen (51 mg) for the complete combustion of 40 mg of DMNB. For HFC experiments at ambient pressure, there was only 1.4 mg of oxygen, which was insufficient to oxidize DMNB significantly. For the DSC microampoule system, where the volume of an ampoule is approximately 5 mm^3, the amount of oxygen in the ampoule was less than 1.4 μg, much smaller than the required amount of oxygen (0.9 mg) for the complete oxidation of 0.7 mg of DMNB. For the ARC system (8 cm^3 internal bomb volume), the amounts of oxygen for experiments started at ambient and 3.5 MPa of air were 2.2 and 76 mg, respectively, and these are less than the required amount (0.31 g) for the complete combustion of 0.25 g of DMNB.

The enthalpy change can be estimated from the initial and final temperatures of the exotherm, and has been determined for the 0.25 g samples at ambient pressure and 3.5 MPa of argon (Table 3). However, the ARC runs started at 3.5 MPa of air were stopped automatically before the exotherm was completed,

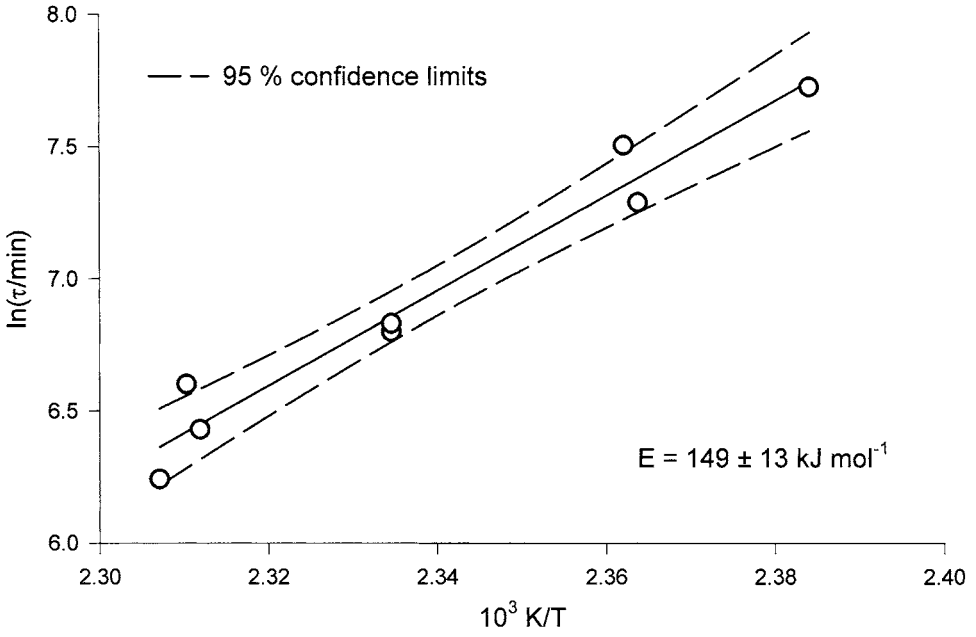

Fig. 10. Kinetic results obtained from isothermal ARC data using time to self-heating rate = 5 K min^{-1}.

because the self-heating rates exceeded the maximum rate of automatic termination (10 K min^{-1}).

It can also be seen from Table 3 that the enthalpy change obtained from HFC is less than that obtained from the DSC microampoule system. The difference can be attributed to the volatility of DMNB. As discussed by Jones et al. [27], the HFC system has a larger free volume, and some of the DMNB sublimes prior to the chemical reaction. This leads to a larger difference in the heat capacity before and after the reaction. Consequently, the uncertainty in the enthalpy values derived from the HFC experiments is larger than those obtained by DSC.

3.2.2. *Decomposition of DMNB in mesitylene solution*

To eliminate the interference of the fusion endotherm, DSC experiments were conducted using mesitylene solutions with 20, 30 and 50 mass % DMNB. The DSC results for 20 % DMNB solutions are illustrated in Fig. 11. The onset temperature for the decomposition is 486 ± 5 K. The enthalpy change of 436 ± 12 kJ mol^{-1} for the decomposition is independent of both heating rate and solution concentration, but is significantly less exothermic than that determined for pure DMNB, suggesting a difference in the final products for the two cases. Independent studies of thermal decomposition of DMNB in mesitylene solution have shown that the products are nitrous acid, a diene and an allylic nitro compound [28]. As shown in Fig. 12, the peak temperature was found to be concentration dependent. Since the peak temperature is inversely proportional to the rate, the rate may increase with concentration of DMNB.

Dynamic and isothermal DSC studies were conducted to determine the kinetic parameters of 20 mass % DMNB in mesitylene solution. Jones and Augsten [4] have analyzed dynamic and isothermal results using ASTM E 698 [21] and Eq. (1), respectively. The isothermal DSC results conducted between 503 and 523 K were also analyzed using the autocatalytic model of Eq. (2). An Arrhenius plot of the rate constants derived from these experiments is shown in Fig. 13 and the kinetic parameters are summarized in Table 4.

The DSC results were also analyzed using the IsoKin isoconversional data analysis program [22] and the results are shown in Fig. 6. The average value of the activation energy obtained over the range $0.3 < \alpha < 0.7$ (Table 4) is similar to that found by ASTM E 698.

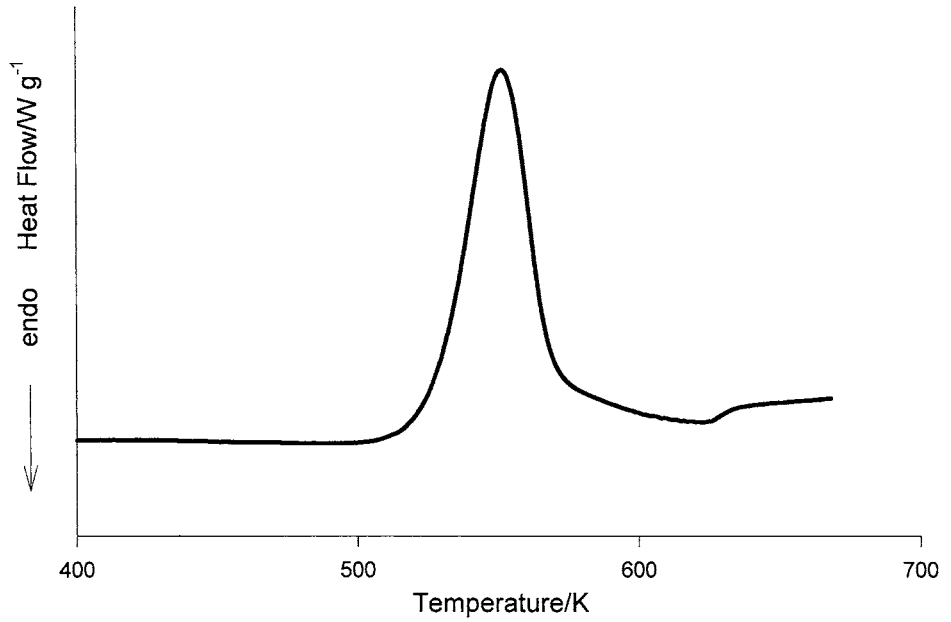

Fig. 11. DSC results for 20 % DMNB solution at $\beta = 10\ \mathrm{K\ min^{-1}}$.

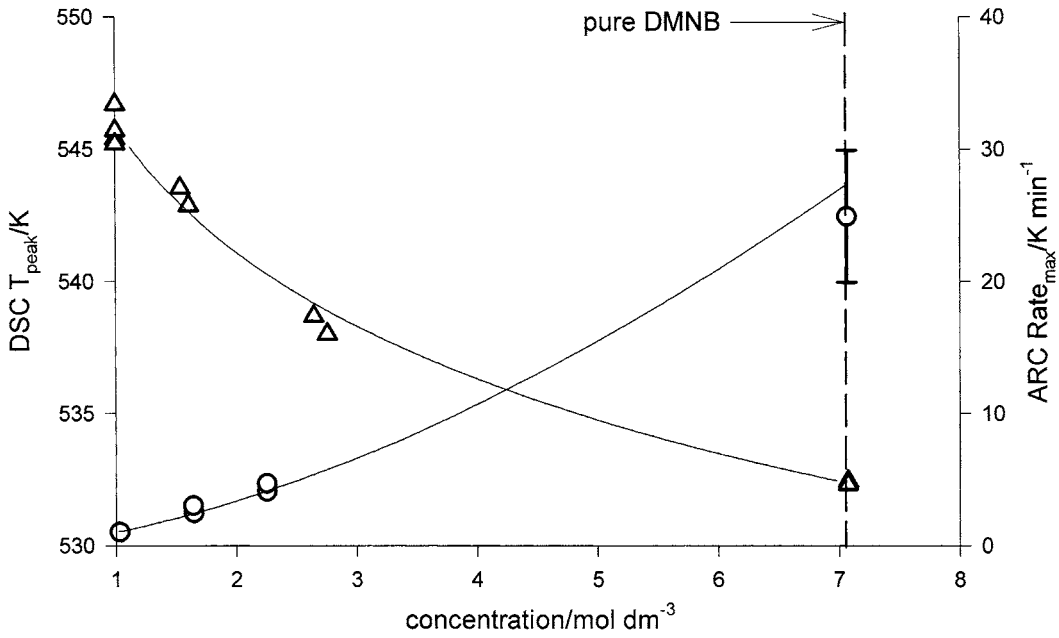

Fig. 12. Comparison of 20, 30 and 50 % DMNB solution. DSC peak temperature, (△); ARC maximum rate, (○).

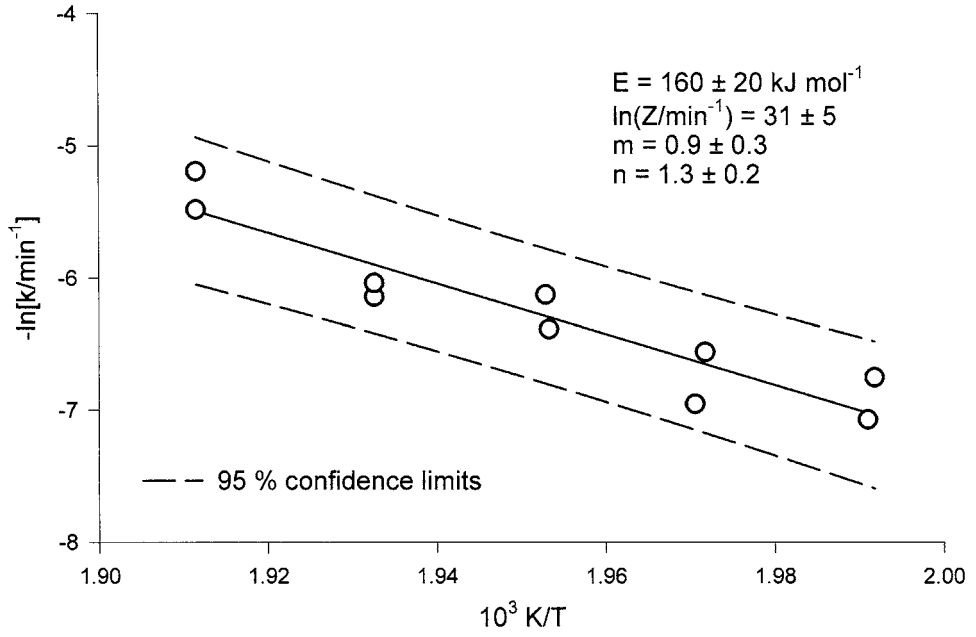

Fig. 13. Isothermal DSC results for 20 % DMNB solution according to Eq. (2).

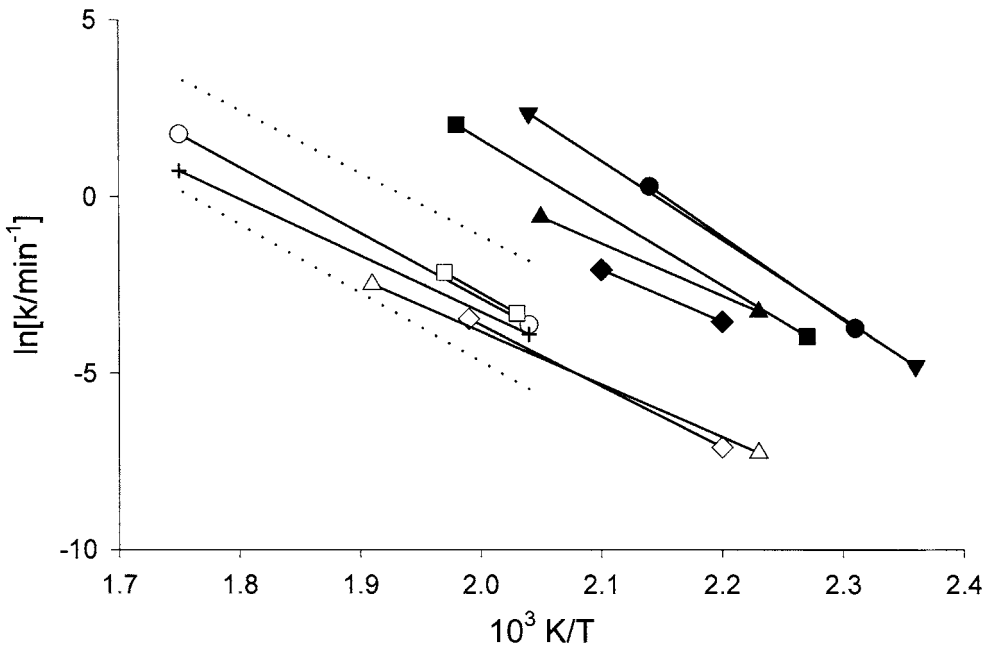

Fig. 14. Comparison of rate constants for various methods. Dynamic DSC, (○); isothermal DSC Eq. (1), (□); ARC Eq. (3) 0.25 g in ambient Ar, (◇); ARC Eq. (3) 0.25 g in ambient air and 3.5 MPa Ar, (△); ARC linear 0.25 g in ambient Ar, (◆); ARC linear 0.5 g in ambient Ar, (■); ARC linear 1.5 g in ambient Ar, (●); ARC linear 0.25 g in ambient air, (▲); ARC linear 0.25 g in 3.5 MPa air, (▼); dynamic DSC for 20 % DMNB solution, (+). Dashed line: uncertainty for dynamic DSC data.

The ARC results for the solutions of 20, 30 and 50 mass % DMNB in mesitylene have been reported previously [4]. The onset temperature of 457 ± 3 K is independent of concentration and is in good agreement with the onset temperature observed for solid DMNB using ARC. As shown in Fig. 12, the maximum rate is concentration dependent. The kinetic parameters for 20 mass % DMNB in mesitylene solution are shown in Table 4.

3.2.3. Comparison of kinetic parameters

Kinetic parameters determined for neat DMNB and DMNB in solution are compared in Table 4. The rate constants for the decomposition of DMNB, calculated using the kinetic parameters in Table 4 over the appropriate temperature range, are compared in Fig. 14. For neat DMNB, the dynamic and isothermal (*n*th-order) DSC results agree with the ARC results (for ambient air, ambient and high-pressure of Ar) analyzed using Eq. (3). For the ARC results analyzed using only the linear region, significantly different rate constants were obtained. It may not be appropriate to compare the ARC linear data to those obtained from Eq. (3). Comparison of the rate constants from the ARC linear data for different sample masses shows that the decomposition appears to be dependent on sample size. Additionally, significantly different rate constants were obtained for DMNB at high-pressure of air, due to the oxidation of DMNB.

The dynamic DSC results for 20 mass % DMNB in mesitylene solution are also shown in Fig. 14. Although, there are significant differences in the values of the kinetic parameters and possibly the final products, the calculated rate constants for DMNB(s) and in solution are in agreement within the temperature range studied.

4. Conclusions

The vapor pressure and the enthalpy of sublimation of DMNB were obtained from DSC measurements. Additionally, the enthalpy of sublimation was determined from dynamic and isothermal TG studies. Different enthalpies of sublimation were obtained from DSC and TG, due to the difference in temperature ranges of the studies. The decomposition of neat DMNB and DMNB in mesitylene solution were studied using DSC and ARC. The kinetic parameters for the decomposition were determined by both methods, and there was reasonable agreement between the two sets of results. The effect of pressure of oxidizing and non-oxidizing gas on the thermal behavior of DMNB was studied using DSC and ARC. The ARC results show that DMNB decomposition seems to be independent of the pressure of inert gas. High-pressure of air enhances the oxidation of DMNB as indicated by lower onset temperature and significantly different rate constants.

References

[1] Doc. 9571 ICAO Convention, International Civil Aviation Organization, Montreal, Canada, 1 March 1991.
[2] D.E.G. Jones, R.A. Augsten, K.K. Feng, J. Therm. Anal. 44 (1995) 533.
[3] D.E.G. Jones, R.A. Augsten, K.P. Murnaghan, Y.P. Handa, C.I. Ratcliffe, J. Therm. Anal. 44 (1995) 547.
[4] D.E.G. Jones, R.A. Augsten, in: Proceedings of the 27th Annual Conference of ICT on Energetic Materials and Technology, Karlsruhe, Germany, 25–28 June 1996.
[5] D.E.G. Jones, H.T. Feng, in: Proceedings of the International Autumn Seminar on Propellants, Explosives and Pyrotechnics, Shenzhen, China, 8–11 October 1997.
[6] D.E.G. Jones, P.D. Lightfoot, R.C. Fouchard, Q.S.M. Kwok, in: Proceedings of the 27th International Pyrotechnics Seminar, Grand Junction, CO, 16−21 July 2000.
[7] D.E.G. Jones, P.D. Lightfoot, R.C. Fouchard, Q.S.M. Kwok, in: Proceedings of the 28th North American Thermal Analysis Society Annual Conference, Orlando, FL, 4−6 October 2000.
[8] ASTM E 967, Standard Practice for Temperature Calibration of Differential Scanning Calorimeters and Differential Thermal Analyzers, American Society for Testing and Materials, Philadelphia, PA, USA.
[9] ASTM E 968, Standard Practice for Heat Flow Calibration of Differential Scanning Calorimeters, American Society for Testing and Materials, Philadelphia, PA, USA.
[10] ASTM E 1582–93, Standard Practice for Calibration of Temperature Scale for Thermogravimetry, American Society for Testing and Materials, Philadelphia, PA, USA.
[11] D.I. Townsend, J.C. Tou, Thermochim. Acta 37 (1980) 1.
[12] D.E.G. Jones, R.C. Fouchard, CERL Internal Report Exp. 99, 19 October 1999.
[13] L. Elias, AH–DE/5–WP/17, International Civil Aviation Organization, Montreal, Canada, 23–27 September 1991.
[14] S.P. Smirnov, Y.N. Matiushin, I.Z. Akmetov, AH–DE/8–WP/12, International Civil Aviation Organization, Montreal, Canada, 14–18 February 1994.
[15] ASTM E 1782–96, Standard Test Method for Determining Vapor Pressure by Thermal Analysis, American Society for Testing and Materials, Philadelphia, PA, USA.

[16] ASTM E 2071, Practice for Calculating Heat of Vaporization or Sublimation from Vapor Pressure Data, American Society for Testing and Materials, Philadelphia, PA, USA.
[17] D.E.G. Jones, R.A. Augsten, R.C. Fouchard, H. Feng, CERL Internal Report Exp. 97, 16 November 1997.
[18] P.J.D. Collins, in: Proceedings of the 27th International Pyrotechnics Seminar, Grand Junction, CO, 16−21 July 2000.
[19] E. Ohiyama, P.G. Wahlbeck, Thermochim. Acta 250 (1995) 41.
[20] J.P. Elder, J. Therm. Anal. 49 (1997) 897.
[21] ASTM E 698–79 (Reapproved 1993), Standard Test Method for Arrhenius Kinetic Constants for Thermally Unstable Materials, American Society for Testing and Materials, Philadelphia, PA, USA.
[22] C.A. Wight, IsoKin Isoconversional Data Analysis Program, Version 1.42, Copyright© 2000, Center for Thermal Analysis, University of Utah, Utah.
[23] S. Vyazovkin, J. Comput. Chem. 18 (1997) 393.
[24] S. Vyazovkin, C.A. Wight, J. Phys. Chem. A 101 (1997) 5653.
[25] S. Vyazovkin, C.A. Wight, Chem. Mater. 11 (1999) 3386.
[26] S. Vyazovkin, C.A. Wight, Anal. Chem. 72 (2000) 3171.
[27] D.E.G. Jones, Y.P. Handa, H. Feng, J. Therm. Anal. 53 (1998) 3.
[28] K. Fritzshe, H.D. Beckhaus, C. Rüchardt, Chimica 42 (1988) 106.